NREL National Renewable Energy Laboratory

A national laboratory of the U.S. Department of Energy
Office of Energy Efficiency & Renewable Energy

Innovation for Our Energy Future

A Quantitative Comparison of the Responses of Three Floating Platforms

Conference Paper
NREL/CP-500-46726
March 2010

J. Jonkman
National Renewable Energy Laboratory

D. Matha
University of Stuttgart, Germany (Universitat Stuttgart)

Presented at European Offshore Wind 2009 Conference and Exhibition
Stockholm, Sweden
September 14–16, 2009

NREL is operated for DOE by the Alliance for Sustainable Energy, LLC   Contract No. DE-AC36-08-GO28308

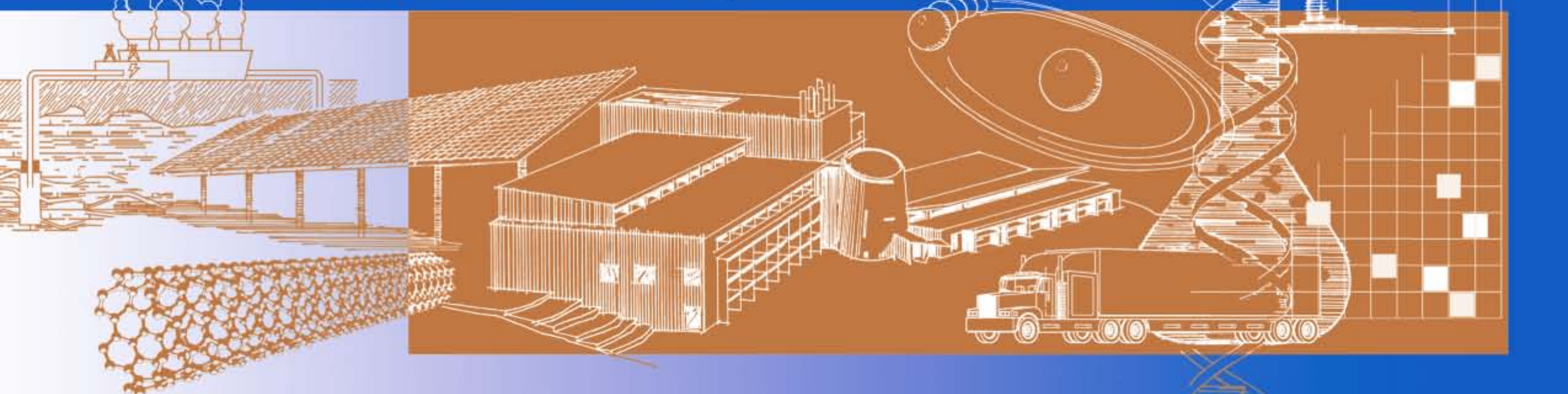

Available electronically at http://www.osti.gov/bridge

Available for a processing fee to U.S. Department of Energy
and its contractors, in paper, from:
U.S. Department of Energy
Office of Scientific and Technical Information
P.O. Box 62
Oak Ridge, TN 37831-0062
phone: 865.576.8401
fax: 865.576.5728
email: mailto:reports@adonis.osti.gov

Available for sale to the public, in paper, from:
U.S. Department of Commerce
National Technical Information Service
5285 Port Royal Road
Springfield, VA 22161
phone: 800.553.6847
fax: 703.605.6900
email: orders@ntis.fedworld.gov
online ordering: http://www.ntis.gov/ordering.htm

Printed on paper containing at least 50% wastepaper, including 20% postconsumer waste

List of Acronyms

CM	center of mass
DEL	damage-equivalent load
DLC	design load case
DOWEC	Dutch Offshore Wind Energy Converter
ECD	extreme coherent gust with direction change
IEA	International Energy Agency
IEC	International Electrotechnical Commision
MIT	Massachusetts Institute of Technology
NREL	National Renewable Energy Laboratory
O & G	oil and gas
O & M	operations and maintenance
OC3	Offshore Code Comparison Collaboration
PSF	partial safety factor
RAO	response amplitude operator
RCC	rainflow-cycle counting
SWL	still water level
TLP	tension leg platform

Executive Summary

This report presents a comprehensive dynamic-response analysis of three offshore floating wind turbine concepts. Models were composed of one 5-MW turbine supported on land and three 5-MW turbines located offshore on a tension leg platform, a spar buoy, and a barge. A loads and stability analysis adhering to the procedures of international design standards was performed for each model using the fully coupled time-domain aero-hydro-servo-elastic design code FAST with AeroDyn and HydroDyn. The concepts are compared based on the calculated ultimate loads, fatigue loads, and instabilities. The results of this analysis will help resolve the fundamental design trade-offs between the floating-system concepts.

Table of Contents

1 Introduction

Currently, most offshore wind turbines are installed in shallow water on bottom-mounted substructures. These substructures include gravity bases used in water to about 10-m depth, fixed-bottom monopiles used in water to about 30-m depth, and space-frames—such as tripods and lattice frames (e.g., "jackets")—used in water to about 50-m depth. In contrast, harnessing much of the vast offshore wind resource potential of the United States, China, Japan, Norway, and many other countries requires installations to be located in deeper water. At some depth, floating support platforms will be the most economical type of support structure to use.

Numerous floating support-platform configurations are possible for use with offshore wind turbines, particularly when considering the variety of mooring systems, tanks, and ballast options used in the offshore oil and gas (O & G) industry. The platforms, however, can be classified in terms of how they achieve basic static stability in pitch and roll. The three primary concepts are the tension leg platform (TLP), spar buoy, and barge; these platforms provide restoring moments primarily by the mooring system combined with excess buoyancy in the platform, a deep draft combined with ballast, and a shallow draft combined with waterplane area moment, respectively. Hybrid concepts, such as semisubmersibles, which use restoring features from all three classes, are also a possibility.

The offshore O & G industry has demonstrated the long-term survivability of offshore floating structures, so, the technical feasibility of developing offshore floating wind turbines is not in question. Developing cost-effective offshore floating wind turbine designs that are capable of penetrating the competitive energy marketplace, however, requires considerable thought and analysis. Transferring the offshore O & G technology directly to the offshore wind industry without adaptation is not economical. These economic challenges impart technological challenges, including:

- The introduction of very low frequency modes that can impact the aerodynamic damping and stability of the system;
- The possibility of significant translational and rotational motions of the support structure, which can couple with the motions of the rotor-nacelle assembly;
- The support structure need not be slender and cylindrical, such that hydrodynamic radiation, diffraction, and other wave effects can become important;
- The mooring and anchoring system is a new component (not found in bottom-mounted offshore substructures) that must be considered in the overall design and analysis; and
- The potential for complicated construction, installation, operations and maintenance (O & M), and decommissioning procedures.

Table 1 presents a qualitative assessment of the relative advantages ("+") and disadvantages ("–") of the three primary offshore wind turbine floating-platform classes with respect to the technological challenges ("0" being neutral). A more detailed qualitative assessment is given in Reference 1.

Table 1. Qualitative Assessment of Offshore Wind Turbine Floating Platform Classes

	TLP	Spar Buoy	Barge
Pitch stability	Mooring	Ballast	Buoyancy
Natural periods	+	0	–
Coupled motion	+	0	–
Wave sensitivity	0	+	–
Turbine weight	0	–	+
Moorings	+	–	–
Anchors	–	+	+
Construction	–	–	+
O & M	+	0	–

To quantify the comparison between the platform classes—which is needed to resolve the fundamental design trade-offs between them—requires detailed design and analysis. To begin the process of making such a quantified comparison, this report presents detailed dynamic-response analyses of four systems: One for a wind turbine supported on land, and three for a wind turbine supported offshore independently on the three primary floating platforms.

2 Overview of the Analysis Approach

The overall design and analysis process applied in this project consists of the following steps.

1. Use the same wind turbine specifications—including specifications for the rotor, nacelle, tower, and controller—for each system. (Minor modifications to the specifications are needed in some cases; *see* Step 2.) Likewise, use the same environmental conditions for each analysis—including meteorological (wind) and oceanographic (wave), or "metocean," parameters. Using the same wind turbine specifications and metocean data for all analyses enables an "apples-to-apples" comparison of the systems.
2. Determine the properties of each floater, including the platform and mooring-system designs. To be suitable, each floating platform must be developed specifically to support the rotor, nacelle, and tower of the wind turbine. In some cases, the wind turbine tower might need to be modified in this step to ensure conformity to the platform. Some platforms also require adaptation of the wind turbine control system in this step to avoid controller-induced instabilities of the overall system. For an explanation of the potential instabilities, see Reference 2 and Reference 3.
3. Develop a model of each complete system within a comprehensive simulation tool capable of modeling the coupled dynamic response of the system from combined wind and wave loading. Modeling the dynamic response of land- and sea-based wind turbines requires the application of comprehensive aero-hydro-servo-elastic simulation tools that incorporate integrated models of the wind inflow, aerodynamics, hydrodynamics (for sea-based systems), controller (servo) dynamics, and structural (elastic) dynamics in the time domain in a coupled nonlinear simulation environment.

4. Verify elements of each full system dynamics model from Step 3 by checking its response predictions with responses predicted by a simpler model. When modeling a floating wind turbine, it is advantageous to verify the sophisticated nonlinear time-domain model against a much simpler linear frequency-domain model. Such a comparison can be made in terms of response amplitude operators (RAOs) for excitation by regular waves or in terms of probability distributions for excitation by irregular waves. This step is important for catching errors that could be difficult to identify in the much more exhaustive analysis of Step 5.
5. Using each full system dynamics model from Step 3, perform a comprehensive loads analysis to identify the ultimate loads and fatigue loads expected over the lifetime of the system. Loads analysis involves running a series of design load cases (DLCs) covering essential design-driving situations, with variations in external conditions and the operational status of the turbine. The loads are examined within the primary components of the wind turbine, including the blades, drivetrain, nacelle, and tower—and for the floating system, the mooring lines. Potential unexpected instabilities also can be found in this process.
6. Using the results of Step 5, characterize the dynamic responses of the land- and sea-based systems. Comparing the land-based and sea-based systems responses enables quantification of the impact brought about by the dynamic coupling between the turbine and each floating platform in the presence of combined wind and wave loading. Comparing the responses of the three sea-based systems with each other enables quantification of the impact of the platform configuration on the turbine.
7. Improve each floating system design through design iteration (i.e., iterating on Step 1 through Step 6), ensuring that each of the system components is suitably sized through limit-state analyses. The results of Step 6 can help identify where design modifications must be made to arrive at a suitable design for the floating system. Application of advanced control techniques—such as multi-input, multi-output state-space-based control schemes—can be used in this step to reduce floating-platform-induced system loads, and to mitigate potential changes to the design of the supported wind turbine.
8. Evaluate each system's economics using cost models, including the influences of the turbine design, construction, installation, O & M, and decommissioning. It is likely that the "best" floating wind turbine concept for a given installation site is the concept with the least-expensive lifecycle cost of energy. The results of Step 6 quantify the extent to which the choices in platform configuration impact the turbine loads—and ultimately the turbine design. Economic analysis, furthermore, shows how the design choices impact the resulting cost of energy. For example, economic analysis can quantify to what extent the cost savings due to the simple design, construction, and installation of the barge are balanced by the need for a strengthened turbine.
9. Identify the best features from each concept that, when combined into a hybrid concept, potentially will provide the best overall system-wide characteristics; then repeat Step 1 through Step 8 with the hybrid concept. This step also should assess variations in the wind turbine concept, and consider unconventional features such as lightweight rotors, high power ratings, two blades instead of three, or downwind rotors instead of upwind rotors.

Section 4, Overview of the Analysis Specifications, describes the specifications, data, and procedures used in this project for Step 1, Step 2, and Step 5. The capabilities of the simulation tool within which each model was developed in Step 3 are described next. The work of Step 4 has been completed for each model, but the results are beyond the scope of this report. The results of Step 5 and Step 6 are presented in Section 5, Results and Discussion. Step 7 through Step 9 are left as future work.

3 Simulation Tool Capabilities

This work applies the NREL-developed FAST servo-elastic tool [4], fully coupled with the AeroDyn rotor aerodynamics module [5] and HydroDyn platform hydrodynamics module [3,6] to enable coupled nonlinear aero-hydro-servo-elastic analysis in the time domain. Turbulent-wind inflow is prescribed by the external computer program TurbSim [7]. FAST and AeroDyn combined account for the applied aerodynamic and gravitational loads, the behavior of the control and protection systems, and the structural dynamics of the wind turbine. The latter contribution includes the elasticity of the rotor and tower, along with the elastic coupling between their motions and the motions of the support platform. Nonlinear restoring loads from the mooring system are obtained from a quasi-static mooring-line module that accounts for the elastic stretching of an array of homogenous taut or slack catenary lines with seabed interaction. The HydroDyn platform hydrodynamics module accounts for linear hydrostatic restoring; nonlinear viscous drag from incident-wave kinematics, sea currents, and platform motion; the added-mass and damping contributions from linear wave radiation, including free-surface memory effects; and the incident-wave excitation from linear diffraction in regular or irregular seas. HydroDyn requires as input hydrodynamic coefficients, including the frequency-domain hydrodynamic-added-mass and hydrodynamic-damping matrices and wave-excitation force vector. In this work, these hydrodynamic coefficients were generated using WAMIT® [8], which uses the three-dimensional numerical-panel method to solve the linearized hydrodynamic radiation and diffraction problems for the interaction of surface waves with offshore platforms in the frequency domain.

4 Overview of the Analysis Specifications

To obtain useful information from this conceptual design-and-analysis project, use of realistic and standardized input data is required. A large collection of input data is needed, including detailed specifications of the wind turbine and floating platforms, along with a design basis. A design basis consists of analysis methods (discussed above), a collection of applicable design standards and load cases, and the site-specific metocean parameters at a reference site. For this project, the specifications of the representative utility-scale multimegawatt turbine known as the “NREL offshore 5-MW baseline wind turbine” were used. The MIT/NREL TLP, the OC3-Hywind spar buoy, and the ITI Energy barge are the floaters used to represent the three primary floating-platform classes. The loads and stability analyses were run according to the procedures of the International Electrotechnical Commission (IEC) 61400-3 offshore wind turbine design standard. A location in the northern North Sea was selected as the reference site from which to obtain metocean data.

4.1 NREL Offshore 5-MW Baseline Wind Turbine

The NREL offshore 5-MW baseline wind turbine is a conventional three-bladed upwind variable-speed variable blade-pitch-to-feather-controlled turbine. The model is based on broad design information from the published documents of turbine manufacturers—with an emphasis on the REpower 5M machine—and on detailed publicly available model properties from other conceptual offshore wind turbine design-and-analysis projects—with an emphasis on the Dutch Offshore Wind Energy Converter (DOWEC) project. The model is derived from a composite of these data, using the best available and most representative specifications. The specifications consist of definitions of the aerodynamic, structural, and control-system properties. Table 2 summarizes some of these properties. Greater detail is provided in Reference 9.

Table 2. Summary of Properties for the NREL 5-MW Baseline Wind Turbine

Rating	5 MW
Rotor orientation, configuration	Upwind, 3 blades
Control	Variable speed, collective pitch
Drivetrain	High speed, multiple-stage gearbox
Rotor, hub diameter	126 m, 3 m
Hub height	90 m
Cut-in, rated, cut-out wind speed	3 m/s, 11.4 m/s, 25 m/s
Cut-in, rated rotor speed	6.9 rpm, 12.1 rpm
Rated tip speed	80 m/s
Overhang, shaft tilt, precone	5 m, 5º, 2.5º
Rotor mass	110,000 kg
Nacelle mass	240,000 kg
Tower mass	347,500 kg
Coordinate location of overall center of mass (CM)	(-0.2 m, 0.0 m, 64.0 m)

4.2 Floating Platforms

The NREL 5-MW system was modeled on the MIT/NREL TLP, the OC3-Hywind spar buoy, and the ITI Energy barge, representing the three primary floating platform classes. All of these floating platforms were developed specifically to support the rotor, nacelle, and tower of the NREL baseline 5-MW system. Using the same turbine system in both the onshore and offshore applications has precedent, because the design process prescribed in the IEC 61400–3 design standard endorses deriving a sea-based wind turbine design from that of a land-based wind turbine.

Each platform is described briefly below. The systems are illustrated in Figure 1 and their properties are summarized in Table 3. Detailed specifications of each design are provided in Reference 10 for the MIT/NREL TLP, Reference 11 for the OC3-Hywind spar buoy, and Reference 3 for the ITI Energy barge.

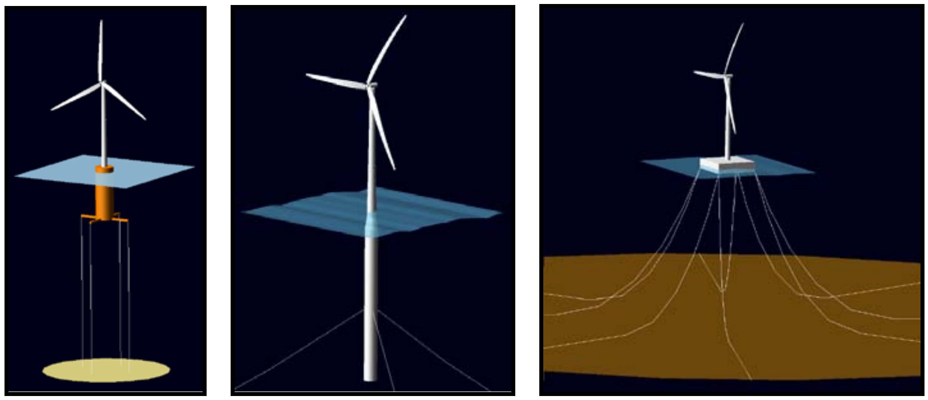

Figure 1. Illustrations of the NREL 5-MW wind turbine on (from left to right) the MIT/NREL TLP, OC3-Hywind spar buoy, and ITI Energy barge

The MIT/NREL TLP is a platform derived from modifications to a TLP designed at the Massachusetts Institute of Technology (MIT). Researchers at MIT have performed a very exhaustive parametric design optimization process using linear frequency-domain solution techniques for TLPs applicable for supporting wind turbines. Modifications were needed, however, to eliminate flaws in the original solution. The resulting TLP—the MIT/NREL TLP—is a cylindrical platform, ballasted with concrete and moored by four pairs of vertical tendons in tension. Each pair of tendons attaches to a spoke that radiates horizontally from the bottom of the platform. The concrete ballast is used to ensure that the combined turbine-platform system remains stable during float-out—even without the tendons—in mild metocean conditions. Note that the platform could have been made much smaller without this design feature. The design of the NREL 5-MW wind turbine remains unchanged when mounted on the MIT/NREL TLP.

The OC3-Hywind spar buoy is a platform that was developed within the Offshore Code Comparison Collaboration (OC3), which is a project that operates under Subtask 2 of the International Energy Agency (IEA) Wind Task 23.[1] The platform imitates the spar-buoy concept called "Hywind," developed by StatoilHydro of Norway,[2] but includes adaptations to make it both suitable for supporting the NREL 5-MW machinery and appropriate for public dissemination. The system is referred to as the "OC3-Hywind" system, to distinguish it from StatoilHydro's original Hywind concept. The OC3-Hywind system features a deeply drafted, slender spar buoy with three catenary mooring lines. The lines attach to the platform via a delta connection (or "crowfoot") to increase the yaw stiffness of the moorings. The tower of the NREL 5-MW wind turbine is modified to conform to the spar, and the baseline generator-torque and blade-pitch controllers are changed to maintain positive aerodynamic damping and to minimize rotor-speed excursions when operating above rated wind speed.

[1] Web page: http://www.ieawind.org/Annex%20XXIII/Subtask2.html (accessed September 11, 2009).
[2] Web page: http://www.statoilhydro.com/en/TechnologyInnovation/NewEnergy/RenewablePowerProduction/Onshore/Pages/Karmoy.aspx (accessed September 11, 2009).

Table 3. Summary of Properties of the Three Floating Platforms

	MIT/NREL TLP	OC3-Hywind Spar Buoy	ITI Energy Barge
Diameter or width × length	18 m	6.5 to 9.4 m (is tapered)	40 m × 40 m
Draft	47.89 m	120 m	4 m
Water displacement	12,180 m^3	8,029 m^3	6,000 m^3
Mass, including ballast	8,600,000 kg	7,466,000 kg	5,452,000 kg
CM location below still water level (SWL)	40.61 m	89.92 m	0.2818 m
Roll inertia about CM	571,600,000 kg • m^2	4,229,000,000 kg • m^2	726,900,000 kg • m^2
Pitch inertia about CM	571,600,000 kg • m^2	4,229,000,000 kg • m^2	726,900,000 kg • m^2
Yaw inertia about CM	361,400,000 kg • m^2	164,200,000 kg • m^2	1,454,000,000 kg • m^2
Number of mooring lines	8 (4 pairs)	3	8
Depth to fairleads, anchors	47.89 m, 200 m	70 m, 320 m	4 m, 150 m
Radius to fairleads, anchors	27 m, 27 m	5.2 m, 853.9 m	28.28 m, 423.4 m
Unstretched line length	151.7 m	902.2 m	473.3 m
Line diameter	0.127 m	0.09 m	0.0809 m
Line mass density	116 kg/m	77.71 kg/m	130.4 kg/m
Line extensional stiffness	1,500,000,000 N	384,200,000 N	589,000,000 N

The ITI Energy barge is a preliminary barge concept developed by the Department of Naval Architecture and Marine Engineering at the Universities of Glasgow and Strathclyde through a contract with ITI Energy. The barge is square and is ballasted with seawater to achieve a reasonable draft, which is not so shallow that it is susceptible to incessant wave slamming. To prevent it from drifting the platform is moored by a system of eight slack, catenary lines. Two of these lines emanate from each corner of the bottom of the barge such that they are 45° apart at the corner. When the NREL 5-MW wind turbine is mounted on the ITI Energy barge, the gains in the baseline blade-pitch controller are detuned to maintain positive aerodynamic damping when operating above rated wind speed.

4.3 Load Cases

A loads and stability analysis was performed for each of the four models, using the IEC 61400-3 offshore wind turbine design standard as a guide. Table 4 summarizes the applied DLCs. In this table, the DLCs are indicated for each design situation by their associated wind conditions; wave conditions; and operational behavior of the control system, fault scenarios, and other events. For the land-based cases the wave conditions were discarded and the tower was cantilevered to the ground at its base.

Simulations considering power production under normal operation throughout a range of wind and wave conditions are considered in the 1.x-series DLCs. The 2.x-series DLC considers power production with fault occurrences, each of which triggers a shutdown of the turbine. The 6.x- and 7.x-series DLCs consider parked (idling) and idling with fault scenarios, respectively, under extreme 1- and 50-year return periods. For DLCs 2.x and 7.x, which involve fault conditions, the IEC standard requires selection of the faults with the worst consequences. The faults in this project were chosen based on common design-driving faults gleaned from experience in other loads analyses. The start-up, normal shutdown, and emergency shutdown events of DLCs 3.x, 4.x, and 5.x—as well as the 8.x-series cases that relate to transport, assembly, maintenance, and repair—are neglected. The IEC 61400-3 standard explains the DLC prescriptions and nomenclature in detail [12]. Reference 3 provides the specifics of how the DLC prescriptions were carried out in this project.

Table 4. Summary of Selected Design Load Cases

DLC	Winds		Waves			Controls / Events	Type	Load Factor
	Model	Speed	Model	Height	Direction			
1) Power Production								
1.1	NTM	$V_{in} < V_{hub} < V_{out}$	NSS	$H_s = E[H_s\|V_{hub}]$	$\beta = 0^\circ$	Normal operation	U	1.25×1.2
1.2	NTM	$V_{in} < V_{hub} < V_{out}$	NSS	$H_s = E[H_s\|V_{hub}]$	$\beta = 0^\circ$	Normal operation	F	1.00
1.3	ETM	$V_{in} < V_{hub} < V_{out}$	NSS	$H_s = E[H_s\|V_{hub}]$	$\beta = 0^\circ$	Normal operation	U	1.35
1.4	ECD	$V_{hub} = V_r$, V_r±2m/s	NSS	$H_s = E[H_s\|V_{hub}]$	$\beta = 0^\circ$	Normal operation; ±Δ wind dir'n.	U	1.35
1.5	EWS	$V_{in} < V_{hub} < V_{out}$	NSS	$H_s = E[H_s\|V_{hub}]$	$\beta = 0^\circ$	Normal operation; ±Δ ver. & hor. shr.	U	1.35
1.6a	NTM	$V_{in} < V_{hub} < V_{out}$	ESS	$H_s = 1.09 \times H_{s50}$	$\beta = 0^\circ$	Normal operation	U	1.35
2) Power Production Plus Occurrence of Fault								
2.1	NTM	$V_{hub} = V_r$, V_{out}	NSS	$H_s = E[H_s\|V_{hub}]$	$\beta = 0^\circ$	Pitch runaway → Shutdown	U	1.35
2.3	EOG	$V_{hub} = V_r$, V_r±2m/s, V_{out}	NSS	$H_s = E[H_s\|V_{hub}]$	$\beta = 0^\circ$	Loss of load → Shutdown	U	1.10
6) Parked (Idling)								
6.1a	EWM	$V_{hub} = 0.95 \times V_{50}$	ESS	$H_s = 1.09 \times H_{s50}$	$\beta = 0^\circ, \pm 30^\circ$	Yaw = 0°, ±8°	U	1.35
6.2a	EWM	$V_{hub} = 0.95 \times V_{50}$	ESS	$H_s = 1.09 \times H_{s50}$	$\beta = 0^\circ, \pm 30^\circ$	Loss of grid → -180° < Yaw < 180°	U	1.10
6.3a	EWM	$V_{hub} = 0.95 \times V_1$	ESS	$H_s = 1.09 \times H_{s1}$	$\beta = 0^\circ, \pm 30^\circ$	Yaw = 0°, ±20°	U	1.35
7) Parked (Idling) and Fault								
7.1a	EWM	$V_{hub} = 0.95 \times V_1$	ESS	$H_s = 1.09 \times H_{s1}$	$\beta = 0^\circ, \pm 30^\circ$	Seized blade; Yaw = 0°, ±8°	U	1.10

Although the IEC 61400-3 standard explicitly states that "the design requirements specified in this standard are not necessarily sufficient to ensure the engineering integrity of floating offshore wind turbines" [12, p. 8], for the purposes of this project (which principally is a conceptual study), the stated design requirements were assumed to be sufficient. No attempt was made to identify other possible floating platform-specific design conditions.

To account for all of the combinations of wind conditions, wave conditions, and control scenarios—together with the number of required seeds—2,190 separate time-domain simulations were run for each offshore floating wind turbine model, and 452 separate simulations were run for the land-based turbine model.

In addition to examining the time-series output from simulations, the simulation data were processed in multiple ways. The statistics (i.e., minimum, mean, and maximum value; standard deviation; skewness; kurtosis) of each output parameter for each simulation were computed. For the ultimate-type (U) simulations, extreme-event tables were generated for each DLC; these tables then were concatenated to find the overall ultimate (maximum) load across all DLCs. Load partial safety factors (PSFs) were applied in this process to weight each DLC properly. For the fatigue-type (F) simulations (DLC 1.2), lifetime damage-equivalent loads (DELs) were calculated according to the process given in the IEC design standards. This process involves (1) binning the cycle ranges and means of each load time series by a rainflow-cycle counting (RCC) algorithm, (2) transforming the load ranges with varying means to equivalent load ranges at a fixed mean load, (3) extrapolating the short-term cycle counts to 20-year lifetime-equivalent cycle counts, and (4) computing the lifetime DEL. In this process the load ranges were transformed from varying to fixed mean loads using a Goodman correction with a range of assumed ultimate strengths. The ultimate strengths were derived by scaling-up the ultimate loads from the land-based loads analysis. The fixed load means were found by weighting the mean loads from each simulation according to the Rayleigh probability distribution at each simulation's associated mean wind speed. The extrapolation for the lifetime-equivalent cycle counts used the same probability distribution. The lifetime DEL was calculated using a range of Wöhler material exponents appropriate to each component. Reference 10 explains the fatigue-processing approach of this project in detail.

When physical (as opposed to numerical) instabilities were found in the load-case simulations, the instabilities were further analyzed using linear system models. The results obtained were consistent with results predicted by the nonlinear time-domain models.

4.4 Reference-Site Data

The location of the former Stevenson Weather Station was selected as the reference site for obtaining environmental (metocean) data. This site is located northeast of the Shetland Islands, which are northeast of Scotland. This site was chosen for its fairly extreme wind and wave conditions, with the implication that the results of the analyses are likely the most severe that would be found at almost any site on Earth. Metocean data at the reference site were purchased through the online service Waveclimate.com,[3] which hosts a worldwide database of wind and wave climate information based on a combination of measurements and a global hindcast model. The resulting data consists of the long-term joint-probability distribution of wind speed, significant wave height, and peak-spectral wave period; as well as the extreme wind speeds, significant wave heights, and peak-spectral wave periods for various return intervals (i.e., 1-year and 50-year return periods). A detailed presentation of the data is provided in Reference 3.

5 Results and Discussion

Loads analyses for each of the four system models were run according to the specifications, data, and procedures described above. Due to the sheer volume of results, only a small fraction can be presented here. The results presented here focus on the characteristic responses of each system and the system-to-system comparisons. Greater detail is available in Reference 3, for the land-based NREL 5-MW wind turbine and the ITI Energy barge system, and in Reference 10 for the MIT/NREL TLP system and the comparison of the three floating wind systems. The loads analyses helped to identify problems with all system configurations, including instabilities in all systems and the susceptibility of excessive platform-pitching motions of the ITI Energy barge in extreme waves. These design problems all led to unacceptably large loadings of the floater-supported wind turbines, which dominated the final predictions in ultimate loads.

Consequently, to gain insight into the dynamic behavior of the onshore and floating systems—and to enable a meaningful comparison between them—the results were split into

[3] Web site: http://www.waveclimate.com/ (accessed September 11, 2009).

groups which are presented separately here. First, the ultimate loads from DLCs 1.1, 1.3, 1.4, and 1.5, which consider the wind turbine in normal operation with a variety of external wind and wave conditions—not including extreme 1- or 50-year events—are presented. Next the fatigue loads from DLC 1.2 are presented. These two sets of results embody the response of the systems unencumbered by the aforementioned design problems. Last, the findings from the other load cases are presented, including those from DLCs 1.6a, 2.x, 6.x, and 7.1a, which are concerned with the wind turbine when it is experiencing a fault, when it is idling, and / or when it is being excited by 1- and 50-year wind and wave conditions. This latter group of results includes a description of the design problems that were identified and possible mitigation measures.

5.1 Ultimate Loads from Design Load Cases 1.1, 1.3, 1.4, and 1.5

The absolute extreme loads from the extreme-event tables (the absolute maximum values of the minima and maxima) of DLCs 1.1, 1.3, 1.4, and 1.5 were calculated. The resulting loads from the three floating wind turbine systems were divided by the corresponding absolute extremes from the land-based turbine's analysis. The resulting dimensionless ratios quantify the impact of installing an NREL 5-MW wind turbine on each of the floating platforms. These ratios are presented in Figure 2 for the bending moments of the blade root, of the low-speed shaft at the main bearing, of the yaw bearing, and of the tower base. A ratio of unity (indicated by the dashed horizontal line) implies that the ultimate load is unaffected by the dynamic couplings between the turbine and the floating platform in the presence of combined wind and wave loading. Ratios greater than unity imply an increase in load or response that might have to be addressed by modifying the system designs (e.g., strengthening the tower) in subsequent analysis iterations. The comparison shows that all the floating wind turbines show increased loads on turbine components as compared to the land-based system.

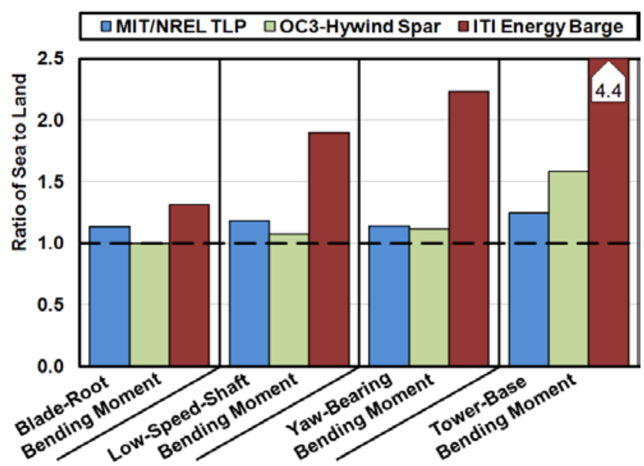

Figure 2. Sea-to-land ratios of ultimate loads from DLCs1.1, 1.3, 1.4, and 1.5

For the land-based wind turbine, many of the greatest loads on the blades and shaft were generated by the extreme coherent gust with direction changes (ECD) of DLC 1.4. The extreme turbulence of DLC 1.3—particularly for mean wind speeds near rated speed—played a significant role in driving most of the other large loads in the system, including the loads in the tower. This is a result of a peak in rotor thrust at rated wind speed, which is characteristic of a pitch-to-feather-controlled wind turbine.

The wind turbine mounted on the ITI Energy barge was affected more by the waves than by the wind. Consequently, DLC 1.1 for the ITI Energy barge system—which has the greater effective partial safety factor for loads—dominated the load results more than did DLC 1.3, which has greater levels of wind but has the same wave conditions. The excessive pitching and rolling motions of the barge bring about load excursions in the supported wind turbine that exceed those experienced by the turbine installed on land. The load excursions become more extreme farther down the load path—from the blade, through the drivetrain and nacelle, to the tower—because of the increased effect of inertia from the barge-pitch motion. The loads are further exacerbated by greater yaw errors between the nominal wind direction and the rotor axis in the ITI Energy barge system as compared to the land-based system. Greater yaw errors allow for more excitation in the side-to-side direction because there is little aerodynamic damping. The greater yaw errors are generated by the yaw motion of the barge. That motion is excited by a gyroscopic yaw moment resulting from the spinning inertia of the rotor in combination with the pitching motion of the barge. Greater yaw motions are generated because of the yaw compliance of the mooring system.

The MIT/NREL TLP system has much less platform motion than does the ITI Energy barge, particularly pitch and roll. The ultimate blade and shaft loads in the MIT/NREL TLP system for the most part were generated by the same DLC that produced the ultimate blade and shaft loads in the land-based wind turbine (DLC 1.4). The loads in the MIT/NREL TLP-supported wind turbine are slightly greater than those of the land-based turbine due to the limited platform motions that do remain. These platform-motion-induced loads cause the design-driving load case to change to DLC 1.1 for the MIT/NREL TLP-based tower as compared to DLC 1.3 for the land-based tower.

The OC3-Hywind spar system has much less pitch and roll motion than that of the ITI Energy barge system, but it has much greater pitch and roll motions than that of the MIT/NREL TLP system. Regarding yaw, the OC3-Hywind spar system is more stable than the MIT/NREL TLP. This yields generally greater shaft and tower loads in the OC3-Hywind system than in the MIT/NREL TLP system, except for loads primarily affected by platform yaw. As compared with the land-based system, DLC 1.4 had much less influence on the blades in the OC3-Hywind system due to the changes in the turbine control system. Instead, most of the ultimate loads in the OC3-Hywind system were driven by DLC 1.3.

In relation to DLCs 1.1, 1.3, and 1.4, DLC 1.5—which considers transient wind-shear events—did not play a significant role in driving ultimate loads for either the land- or sea-based wind turbine systems.

Although mooring loads are not quantified here, the greatest mooring-line tensions in the slack, catenary lines of the OC3-Hywind and ITI Energy barge systems—particularly at the anchors and fairleads of the upwind mooring lines—were driven by simulations involving sustained winds at or near rated wind speed. This is because sustained winds at rated speed generate the greatest sustained rotor-thrust forces, which push the platforms downwind (in surge) and tug on the upwind mooring lines. In the MIT/NREL TLP, the minimum line tension—particularly for the downwind lines, which have less tension than the upwind lines due to the moment countering the rotor thrust—is far more important than the maximum tension because the lines are prone to snap if they transition from their natural taut state to slack and then back to taut. The minimum tensions in the MIT/NREL TLP were caused by simulations with the highest waves—near cut-out wind speed—which induced the greatest platform-pitch motions. Even in these cases, however, the lines remained safely in tension.

5.2 Fatigue Loads from Design Load Case 1.2

Figure 3 presents the ratios calculated by dividing the lifetime DELs for the three investigated floating wind turbine concepts by the corresponding lifetime DELs from the land-based analysis. Ratios are given for the in-plane and out-of-plane blade-root bending moments, the 0° and 90° low-speed-shaft bending moments at the main bearing, and the side-to-side and fore-aft bending moments in the yaw bearing and in the tower base. Each DEL is computed using multiple Wöhler material exponents (m). For the composite blade, the DELs are computed using m equal to 8, 10, and 12. For the steel shaft tower, the DELs are computed using m equal to 3, 4, and 5. Although the DELs also were calculated using a range of ultimate strengths, Figure 3 presents only the results calculated with the greatest ultimate strengths applied. (The DELs asymptotically approach a constant value as the ultimate strength is increased; *see* Reference 10).

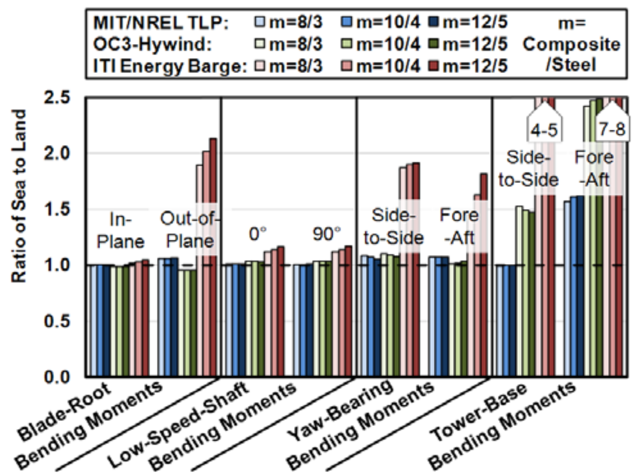

Figure 3. Sea-to-land ratios of fatigue loads from DLC 1.2

In general, the fatigue load ratios show similar trends to those of the ultimate load ratios, and are produced by the same physics explained for the ultimate loads. The fatigue loads of the ITI Energy barge-supported wind turbine are by far the greatest for all of the concepts—particularly for the blade and tower. The fatigue loads in the blade of the OC3-Hywind system are, perhaps surprisingly, less than those of the land-based system. This is a result of the controller modification in the OC3-Hywind system, which trades reduced blade loading for increased shaft loading. The differences in the fatigue loads between the MIT/NREL TLP system and the OC3-Hywind system are not significant, however, except for the fatigue loads of the tower base, which are greater in the OC3-Hywind system.

It should be noted that the nonlinear nature of the fatigue calculation implies that small changes in the DEL can have a great influence on the resulting fatigue lifetime. The fatigue lifetimes for each concept are presented in Reference 10.

5.3 Other Load Cases and Instabilities

The loads analyses of DLCs 1.6a, 2.x, 6.x, and 7.1a—which are concerned with the wind turbine when it is experiencing a fault, when it is idling, and when it is being excited by 1-year and 50-year wind and wave conditions—helped to identify problems with all system configurations. These design problems led to wind turbine loadings that were unacceptably large, and therefore are not quantified here. A qualitative summary is presented instead.

The first problem identified was a coupled blade-edge and tower side-to-side bending instability in the land-based wind turbine. Instability means that some modes of the system have negative damping. The instability occurs when the turbine idles with all blades fully feathered to the maximum pitch setting of 90º, but only when the rotor is positioned at certain azimuth angles and is misaligned with the mean wind direction by 20º to 40º on either side of 0º. The instability was identified when analyzing the loads predicted by DLC 6.2a—which considers extreme 50-year wind conditions. Upon further inspection, the instability also was found to occur at lesser wind speeds, but it is more severe at the greater wind speed. The instability leads to excessive limit-cycle oscillations in the blade-edge and tower side-to-side displacements and loads. Because the MIT/NREL TLP and OC3-Hywind systems respond like the land-based system in many cases, it is not surprising that a similar instability also was found in these floating systems. The floating systems, however, were found to have negative damping in additional system modes, including platform roll and yaw. In a fascinating result, the instability was found to be diminished in the ITI Energy barge system because of barge-induced wave-radiation damping.

This side-to-side instability is caused by an aero-elastic interaction. Although the exact cause has not been determined, what is known about the instability suggests three possible remedies.

- Modify the shape of the airfoils in the blades to reduce the amount of energy absorption at the problematic angles of attack.
- Apply a fail-safe shaft brake to park the rotor in extreme winds and keep it from reaching the critical azimuth positions.
- Allow a slip in the nacelle-yaw drive to keep the rotor away from the critical yaw misalignments.

The downside of the last two potential solutions is that they could cause excessive wear on the shaft brake and nacelle-yaw drive, respectively, which could create a need for routine maintenance.

The second problem identified was a platform-yaw instability in the MIT/NREL TLP and ITI Energy barge systems. The instability occurs when the rotor is idling with a fault, where one blade (the faulted blade) is seized at the minimum pitch set point of 0º and the other two blades are fully feathered to the maximum pitch setting of 90º. This fault event occurs in both DLC 2.1 and 7.1a, but is more severe in DLC 7.1a due to the more extreme (1-year) wind and wave conditions. The instability is caused by an aero-elastic coupling of the platform-yaw motion with the azimuthal motion of the seized blade, and leads to excessive limit-cycle oscillations in the platform-yaw displacement. This, in turn, can cause knotting of the mooring lines, excessive loading of the wind turbine from the ensuing dynamics, or both.

As in the case of the side-to-side instability, the exact cause of this problem has not been determined, but what is known about the platform-yaw instability suggests three possible remedies.

- Supplement the yaw damping by installing damping plates below the free surface. In the OC3-Hywind system, for example, the hydrodynamic damping in yaw is high enough that the platform-yaw instability only occurs in wind conditions greater than the 1-year return wind speeds (the IEC 61400-3 design standard does not require consideration of this factor with this fault condition).
- Apply a fail-safe shaft brake to park the rotor when shut down.

- Reduce the pitch angle of the fully feathered blades to generate a low but persistent aerodynamic torque that produces a slow roll of the rotor while idling.

The latter two solutions would prevent the seized blade from coupling with the platform-yaw motion.

The final problem identified by the loads analyses was that the ITI Energy barge is susceptible to excessive motions when the incident waves are large or steep, such as during extreme 1-year or 50-year wave conditions. This is especially true with the harsh conditions that occur at the chosen reference site. The problems exist whether the wind turbine is idling, as in DLCs 6.x and 7.1a, or producing power, as in DLC 1.6a. The response is more extreme, however, in the idling turbine because the operating turbine introduces more aerodynamic damping. More likely than not, unless the barge is installed only at sheltered sites, modifications to the system design will be required to eliminate the vulnerability of the barge to extreme waves. Possibilities include streamlining the shape of the barge to allow surface waves to pass more easily (e.g., as for a spar buoy), introducing tauter mooring lines (e.g., as for a TLP), or introducing articulated joints to eliminate the direct coupling between the motions of the barge and the turbine.

6 Conclusions

The results presented in this report characterize the dynamic responses of the three primary floating wind turbine concepts, represented here by the MIT/NREL TLP, the OC3-Hywind spar buoy, and the ITI Energy barge system, together with the NREL 5-MW baseline wind turbine. The impacts brought about by the dynamic coupling between the turbine and each floating platform are presented, and comparisons between the concepts are quantified. In summary, all of the floating wind turbines show increased loads on turbine components as compared to the land-based system, and therefore they must be strengthened. The platform motion-induced ultimate and fatigue loads for all turbine components in the ITI Energy barge are by far the greatest loads found for the three concepts. The differences in the ultimate and fatigue loads between the MIT/NREL TLP system and the OC3-Hywind system are not significant, except for the loads in the tower, which are greater in the OC3-Hywind system. Instabilities in all systems also must be resolved.

These results will help resolve the fundamental design trade-offs between the floating system concepts. Although the present results quantify the extent by which the choices in platform configuration impact the turbine loads and ultimately the turbine design, without further considerations (especially economic), no definite statement can yet be made about which concept or hybrid thereof is likely the “best.” Future work will be aimed at model improvements, design iteration, application of advanced control, cost modeling, and the analysis of other floating wind turbine concepts, including variations in platform and wind turbine configuration. If the technical challenges can be solved in an economically feasible way, then the possibility of using offshore floating wind turbines to power much of the world with an indigenous, nonpolluting, and inexhaustible energy source can become reality.

7 References

1. Butterfield, S.; Musial, W.; Jonkman, J.; Sclavounos, P.; Wayman, L. "Engineering Challenges for Floating Offshore Wind Turbines." *Copenhagen Offshore Wind 2005 Conference and Expedition Proceedings, 26–28 October 2005, Copenhagen, Denmark* [CD-ROM], Copenhagen, Denmark: DWIA, October 2005; NREL/CP-500-38776. Golden, CO: National Renewable Energy Laboratory.

2. Larsen, T.J.; Hanson, T.D. "A Method to Avoid Negative Damped Low Frequent Tower Vibrations for a Floating, Pitch Controlled Wind Turbine." *Journal of Physics: Conference Series, The Second Conference on the Science of Making Torque from Wind, Copenhagen, Denmark, 28–31 August 2007* [online journal], 012073, Vol. 75, 2007, URL: http://www.iop.org/EJ/article/1742-6596/75/1/012073/jpconf7_75_012073.pdf?request-id=SpEuhRBu3BG0xV3r2wi7Kg, [cited 28 August 2007]; DOI: 10.1088/1742-6596/75/1/012073.

3. Jonkman, J.M. *Dynamics Modeling and Loads Analysis of an Offshore Floating Wind Turbine*. Ph.D. Thesis. Department of Aerospace Engineering Sciences, University of Colorado, Boulder, Colorado, 2007; NREL/TP-500-41958. Golden, CO: National Renewable Energy Laboratory.

4. Jonkman, J.M.; Buhl Jr., M.L. *FAST User's Guide*. NREL/EL-500-38230. Golden, CO: National Renewable Energy Laboratory, 2005.

5. Laino, D.J.; Hansen, A.C. *User's Guide to the Wind Turbine Dynamics Aerodynamics Computer Software AeroDyn*. Salt Lake City, UT: Windward Engineering LLC, December 2002.

6. Jonkman, J.M. "Dynamics of Offshore Floating Wind Turbines—Model Development and Verification." *Wind Energy*, Vol. 12, No. 5, July 2009, pp. 459–492; DOI: 10.1002/we.347.

7. Jonkman, B.J.; Buhl Jr., M.L. *TurbSim User's Guide*. NREL/EL-500-41136, Golden, CO: National Renewable Energy Laboratory, 2007.

8. Lee, C.H.; Newman, J.N. *WAMIT® User Manual, Versions 6.3, 6.3PC, 6.3S, 6.3S-PC*. Chestnut Hill, MA: WAMIT, Inc., 2006.

9. Jonkman, J.; Butterfield, S.; Musial, W.; Scott, G. *Definition of a 5-MW Reference Wind Turbine for Offshore System Development*. NREL/TP-500-38060. Golden, CO: National Renewable Energy Laboratory, 2009.

10. Matha, D. *Model Development and Loads Analysis of an Offshore Wind Turbine on a Tension Leg Platform, with a Comparison to Other Floating Turbine Concepts*. M.S. Thesis, University of Stuttgart, Germany, 2009; NREL/TP-500-45891. Golden, CO: National Renewable Energy Laboratory.

11. Jonkman, J. *Definition of the Floating System for Phase IV of OC3*. Golden, CO: National Renewable Energy Laboratory, July 2009 (forthcoming).

12. International Electrotechnical Commission. IEC 61400–3 Ed. 1. *Wind Turbines—Part 3: Design Requirements for Offshore Wind Turbines*. Geneva, Switzerland: International Electrotechnical Commission, 2008.

REPORT DOCUMENTATION PAGE

Form Approved
OMB No. 0704-0188

1. REPORT DATE *(DD-MM-YYYY)*	2. REPORT TYPE	3. DATES COVERED *(From - To)*
March 2010	Conference Paper	September 14-16, 2009

4. TITLE AND SUBTITLE
A Quantitative Comparision of the Responses of Three Floating Platforms

5a. CONTRACT NUMBER
DE-AC36-08-GO28308

5b. GRANT NUMBER

5c. PROGRAM ELEMENT NUMBER

6. AUTHOR(S)
J. Jonkman and D. Matha

5d. PROJECT NUMBER
NREL/CP-500-46726

5e. TASK NUMBER
WE10.1211

5f. WORK UNIT NUMBER

7. PERFORMING ORGANIZATION NAME(S) AND ADDRESS(ES)
National Renewable Energy Laboratory
1617 Cole Blvd.
Golden, CO 80401-3393

8. PERFORMING ORGANIZATION REPORT NUMBER
NREL/CP-500-46726

9. SPONSORING/MONITORING AGENCY NAME(S) AND ADDRESS(ES)

10. SPONSOR/MONITOR'S ACRONYM(S)
NREL

11. SPONSORING/MONITORING AGENCY REPORT NUMBER

12. DISTRIBUTION AVAILABILITY STATEMENT
National Technical Information Service
U.S. Department of Commerce
5285 Port Royal Road
Springfield, VA 22161

13. SUPPLEMENTARY NOTES

14. ABSTRACT *(Maximum 200 Words)*
This report presents a comprehensive dynamic-response analysis of three offshore floating wind turbine concepts. Models were composed of one 5-MW turbine supported on land and three 5-MW turbines located offshore on a tension leg platform, a spar buoy, and a barge. A loads and stability analysis adhering to the procedures of international design standards was performed for each model using the fully coupled time-domain aero-hydro-servo-elastic design code FAST with AeroDyn and HydroDyn. The concepts are compared based on the calculated ultimate loads, fatigue loads, and instabilities. The results of this analysis will help resolve the fundamental design trade-offs between the floating-system concepts.

15. SUBJECT TERMS
offshore floating wind turbine, dynamic response analysis, offshore turbine, tension leg platform, spar buoy, barge, loads analysis, stability analysis, aero-hydro-servo-elastic design code FAST

16. SECURITY CLASSIFICATION OF:			17. LIMITATION OF ABSTRACT	18. NUMBER OF PAGES	19a. NAME OF RESPONSIBLE PERSON
a. REPORT	b. ABSTRACT	c. THIS PAGE			
Unclassified	Unclassified	Unclassified	UL		19b. TELEPHONE NUMBER *(Include area code)*

Standard Form 298 (Rev. 8/98)
Prescribed by ANSI Std. Z39.18

F1147-E(10/2008)